ISSN 1009 – 3095 *Journal of Zhejiang University SCIENCE* V.3, No.1, P.13 – 18, Jan. – Mar., 2002
http://www.periodicals.com.cn; http://www.zju.edu.cn/depart/zdxb
http://lib.zju.edu.cn/eindex.htm; http://www.zjupress.com; jzu_s@mail.hz.zj.cn

Stress field near an interface edge of linear hardening materials*

XU Jin-quan(许金泉)†, FU Lie-dong(付列东)

(*Department of Mechanics, Zhejiang University, Hangzhou, China, 310027*)

Received Jan. 18, 2001; revision accepted Apr.18, 2001

† Email: jinquan@mech.nagaokaut.ac.jp

Abstract: The elastic-plastic singular stress field near an interface edge of bounded linear hardening material is substantially as same as that of bonded elastic materials whose Young's modulus and Poisson ratio are substituted by equivalent values, respectively. Further investigation by the elasto-plastic boundary element method (BEM) on the stress field near the interface edge showed that the stress field there can be divided into three regions: the domain region of the elastic-plastic singular stress field, the transitional region and the elastic region. The domain region of the elastic-plastic singular stress becomes larger with the increasing of the linear hardening coefficient. When the linear hardening coefficient decreases to a certain value, the effective stress in most of the yield zone equals approximately the yield stress. The stress distribution in the elastic region under small-scale yielding condition was also investigated.

Key words: interface edge, elastoplasticity, linear hardening, singularity, boundary element method
Document code: A **CLC number:** TB125, O344.3

INTRODUCTION

In recent years, bonded materials have been widely used in electronic devices, metal/ceramic joints and composites engineering. The linear elastic interfacial mechanics, which is based on elasticity and developed in the last 20 years, is a useful tool to evaluate the strength of bonded dissimilar material structures. It is well known that stresses near an interface edge may become singular, based on elastic theory. Due to the stress singularity, the material will yield near the interface edge, and the elastic analysis results may not be applicable, especially when the yield strength of the composed material is low. Therefore, elastic-plastic analysis is necessary for the evaluation of such a bonded dissimilar material. Shih and Asaro (1988, 1989, 1991) investigated the elastic-plastic behaviores of an interface crack by finite element method (FEM) analysis. Gao and Lou (1990), Xia and Wang (1992), and Champion and Atkinson (1990, 1991) analyzed the asymptotic singular stress field near an interface crack tip. Rudge and Tiernan (1995) analyzed the elastic plastic stress singularity near the interface edge for the case when hardening exponents of the bonded power law hardening materials are the same.

For linear hardening material, Xu and Mutoh (1999) gave the elastic-plastic singular stress field near the interface edge of bonded linear hardening materials, based on the linear approximation of the stress-strain relation near the edge. In this paper, a more concise approach was adopted to analyze the theoretical elastic plastic singular stress near the interface edge. The result obtained was much clearer and easier for application. BEM analysis was carried out in order to obtain more detailed characters of the stress distributions near the interface edge. It was found that the elastic plastic singular order obtained numerically agreed with the theoretical results when the hardening coefficient was relatively large, but did not agree if the hardening coefficient was smaller than a certain value.

THEORETICAL ANALYSIS

According to the total strain theory, the strain stress relation of a linear hardening materi-

* Project (No.19972060) supported by the National Natural Science Foundation of China.

al can be expressed as:

$$\varepsilon_{ij} - \delta_{ij}\varepsilon_m = \left[\frac{3}{2H'}\left(1 - \frac{\sigma_y}{\sigma_e}\right) + \frac{1}{2\mu}\right](\sigma_{ij} - \delta_{ij}\sigma_m) \tag{1}$$

Where H' is the hardening coefficient, σ_y is the yield stress, μ is the shear modulus. σ_m is the average stress, σ_e is the effective stress. $\varepsilon_m = \varepsilon_m^e + \varepsilon_m^p$ is the cubic strain, where the superscripts e and p denote the elastic and plastic part respectively. According to the plastic incompressible principle, $\varepsilon_m = \varepsilon_m^e = \dfrac{1-2v}{E}\sigma_m$

Now we consider the elastic plastic stress field near the interface edge as shown in Fig.1.

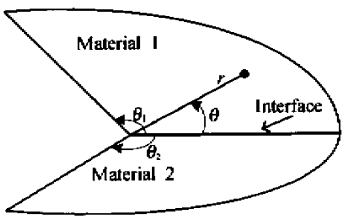

Fig.1 Model of interface edge

If the elastic-plastic stress near the interface edge behaves as singular, then one can always find a region within which $\sigma_y/\sigma_e << 1$ is satisfied, so that Eq.(1) can be simplified to

$$\varepsilon_{ij} - \delta_{ij}\varepsilon_m = \left(\frac{3}{2H'} + \frac{1+v}{E}\right)(\sigma_{ij} - \delta_{ij}\sigma_m) \tag{2}$$

Eq.(2) is in fact the constitutive equation of a linear elastic material. Assuming its Young's modulus and Poisson ratio are E', v' respectively, we have:

$$\varepsilon_{ij} - \delta_{ij}\frac{1-2v'}{3E'}\sigma_{kk} = \frac{1+v'}{3E'}(\sigma_{ij} - \delta_{ij}\sigma_m) \tag{3}$$

Equating the corresponding parts of Eq.(2) with that of Eq.(3), we have

$$\frac{1-2v}{E} = \frac{1-2v'}{E'},\quad \frac{3}{2H'} + \frac{1+v}{E} = \frac{1+v'}{E'} \tag{4}$$

i.e.

$$E' = \frac{EH'}{E+H'},\qquad v' = \left(v + \frac{E}{2H'}\right)/\left(1 + \frac{E}{H'}\right) \tag{5}$$

Therefore, the elastic plastic analysis of linear hardening materials for a problem with a singular point can be carried out as an elastic problem if the material constants are considered on the basis of Eq.(5). The eigenequation to determine the stress singularity can then be given by the analogue with the well-known elastic result of an interface edge (Bogy, 1971) as:

$$A\beta^2 + 2B\alpha\beta + C\alpha^2 + 2D\beta + 2E\alpha + F = 0 \tag{6}$$

where

$$\left.\begin{aligned} A &= 4K(\lambda,\theta_1)K(\lambda,\theta_2)\\ B &= 2\lambda_2\sin^2\theta_1 K(\lambda,\theta_2) + 2\lambda^2\sin^2\theta_2 K(\lambda,\theta_1)\\ C &= 4\lambda_2(\lambda_2 - 1)\sin^2\theta_1\sin^2\theta_2 + K(\lambda,\theta_1+\theta_2)\\ D &= 2\lambda_2[\sin^2\theta_1\sin^2\lambda\theta_2 - \sin^2\lambda\theta_1\sin^2\theta_2]\\ E &= -D + K(\lambda,\theta_2) - K((\lambda,\theta_1) \end{aligned}\right\} \tag{7}$$

$$K(\lambda,\theta) = \sin^2(\lambda\theta) + \lambda^2\sin\theta \tag{8}$$

$$\alpha = \frac{\Gamma(\kappa_1+1) - (\kappa_2+1)}{\Gamma(\kappa_1+1) + (\kappa_2+1)},$$

$$\beta = \frac{\Gamma(\kappa_1-1) - (\kappa_2-1)}{\Gamma(\kappa_1+1) + (\kappa_2+1)} \tag{9}$$

But the material constants κ, Γ should be modified as follows:

$$\kappa = \begin{cases} 3-4v' & \text{for plane strain} \\ (3-v')/(1+v') & \text{for plane stress} \end{cases},$$

$$\Gamma = \mu_2/\mu_1 = \frac{E'_2(1+v'_1)}{E'_1(1+v'_2)} \tag{10}$$

where v' are E' given by Eq.(5). The stress field can also be expressed in a form similar to that of the elastic singular field near an interface edge as

$$\sigma_{ij} \propto r^{\lambda-1} \tag{11}$$

where $\lambda - 1$ corresponds to the elastic plastic singular order.

BEM ANALYSIS MODEL AND GENERAL FEATURES OF ELASTIC PLASTIC STRESS FIELD

The BEM tool is especially efficient and accurate for elastic analysis of bonded dissimilar materials. Considering that traction on the interface can be obtained directly, and that the discretization is only needed for the boundary and the yield zone, BEM can be also considered as

an efficient and accurate tool for elastic plastic analysis of bonded dissimilar materials.

The elastic plastic BEM formulation can be found in many references (e.g., Brebbia, Telles and Wrobel, 1984). We developed a BEM elastic plastic analysis program which has been confirmed to be accurate enough and very efficient. This program based on the incremental strain theory, and adopting the Von-Mises yield condition was used to analyze the Fig.2 model under plane strain condition. For simplicity, material 2 was considered as an ideally elastic material, and material 1 as a linear hardening material.

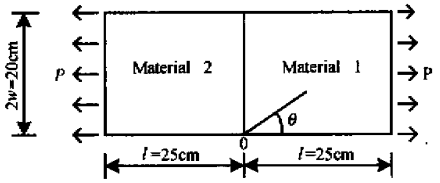

Fig.2 Model of computation

To investigate the general features of the singular elastic plastic stress field, we assume the material constants are: $H' = 1600$MPa, $\sigma_Y = 123$ MPa, $E_1 = 4.93$ GPa, $v_1 = 0.33$, $E_2 = 206$ GPa, $v_2 = 0.30$. The loading is $P = 125$ MPa. It should be noted that the effective stress far from the interface in material 1 is

$$\sigma_e = 0.88P = 110 \text{ MPa} \qquad (12)$$

which is smaller than the yield stress. Considering the symmetry, only half of the model needs to be analyzed. Internal cells near the edge point O are divided as shown in Fig.3.

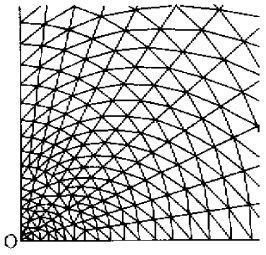

Fig.3 Internal cells

The double logarithmic distribution of the effective stress along the interface is given in Fig.4 in which, the stress field near the interface edge is divided into three regions: region I, the domain region of the singular elastic-plastic stress field within which the double logarithmic stress distribution is linear; region II, the transitional region within which the double logarithmic stress distribution is a curve; and region III, the elastic region in which the effective stress is smaller than the yield stress and the double logarithmic stress distribution may also be linear for the case of small scale yielding. In the domain region of the singular elastic-plastic stress field, the slope of the distribution obviously corresponds to the elastic-plastic stress singular order $(\lambda - 1)$.

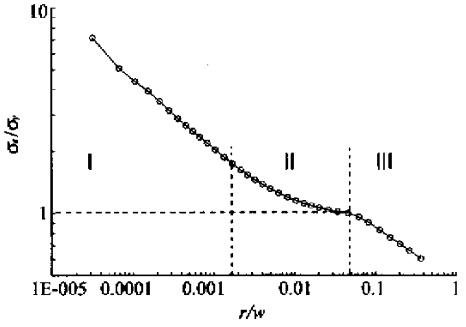

Fig.4 Stress distribution along the interface

The double logarithmic stress distributions in various directions within the domain region are given in Fig.5 showing that the distributions are linear and almost parallel to each other. The slopes (i.e., the singular order) obtained by the least square method and the theoretical elastic-plastic singular order determined by Eq. (6) are given in Table 1 showing that numerical results of the elastic plastic singular order agree well with the analogue results based on linear approximation. This fact indicates that the

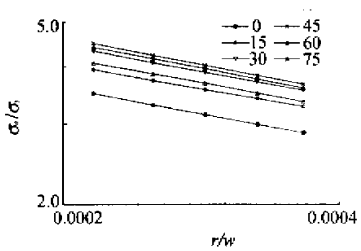

Fig.5 Stress distribution of the interpolation region

stress-strain relation in the domain region can be approximated as linear, and that the singular elastic-plastic stress field can be obtained just by analogue analysis of the elastic interface edge.

Table 1 Numerical results and approximate theoretical solution of the singular order

Direction	15°	30°	45°	60°	75°	90°	Eq.(6)
$\lambda - 1$	−0.3663	−0.3858	−0.3846	−0.3701	−0.3486	−0.3756	−0.3758
Relative Error	2.53%	2.66%	2.34%	1.52%	7.26%	0.05%	

EFFECT OF THE HARDENING COEFFICIENT ON THE SINGULAR FIELD

1. On the singular order

In the previous example, a quite large hardening coefficient was assumed. In this section, we will focus on the effect of the hardening coefficient on the elastic-plastic singular order. We analyzed 6 cases in which the hardening coefficient changed from 1600 MPa ($H'/E = 0.324$) to 50 MPa($H'/E = 0.01$), but the loading condition and other material constants were the same as that of the previous example. Distributions of the effective stress along the interface for various hardening coefficients are given in Fig.6 showing that the effective stress in the yield zone decreases as the hardening coefficient decreases. For the cases with small hardening coefficients, it was found that the effective stress in most part of the yield zone nearly equals to the yield stress. This fact indicates that one can deal with the material with small hardening coefficient as ideal elastic-plastic material. It can also be found that the size of the domain region of the elastic-plastic singular stress is also dependent on the hardening coefficient; the larger the hardening coefficient is, the larger the domain region becomes.

Table 2 shows the singular order for different hardening coefficients. The approximate theoretical results obtained by Eq.(6) are also shown in the table. Collation of Table 2 data with Fig. 7 shows that the numerical results agree well with the approximate theoretical results when $H'/E \geqslant 0.04$, but do not agree with each other when $H'/E < 0.04$. The reason for this can be explained as follows:

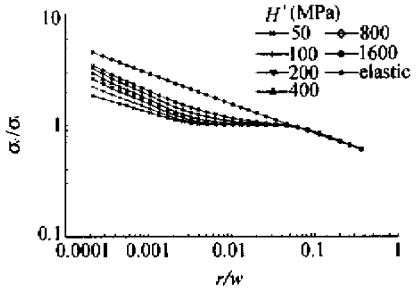

Fig.6 The effective stress distributions along the interface for various hardening coefficients

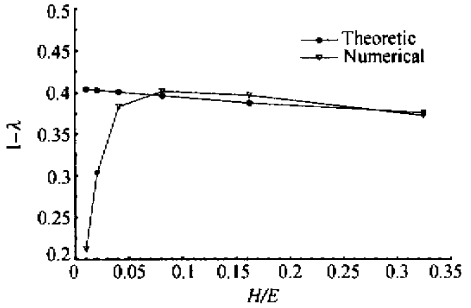

Fig.7 Comparison of numerical and theoretical singular orders

Table 2 Numerical and theoretical results of the singular order for different hardening coefficients

H'(Mpa)	1600	800	400	200	100	50
Theoretical results	−0.3758	−0.3875	−0.3963	−0.4007	−0.4030	−0.4042
Numerical results	−0.3723	−0.3969	−0.4017	−0.3832	−0.3021	−0.2124
Error	0.93%	2.43%	1.36%	4.59%	/	/

In case the material has a small hardening coefficient, in most parts of the yield zone, the effective stress nearly equals to the yield stress, so the condition $\sigma_Y/\sigma_e << 1$ cannot be satisfied

in such a region. This means that the approximate theory is not applicable to such a region, but the numerical result may be calculated from it. From this opinion, it can be expected that the numerical result may agree with the approximate theoretical result if it is determined from the much smaller region near the interface edge by more fine BEM analysis. However, determining the singularity in such a small region may lose its physical meanings.

2. On the shape of the yield zone

To investigate the hardening coefficient's effect on the shape of the yield zone, we also carried out BEM analysis for 6 cases with different hardening coefficients, while the loading was chosen as $P = 30$ MPa. Fig. 8 shows the shapes of the yield zone.

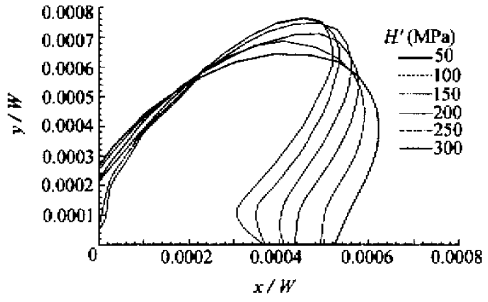

Fig. 8 Shapes of the yield zone for various hardening coefficients when $P = 30$ MPa

It can be found that the yield zone becomes thinner and longer; and the direction of the largest yield radius approaches to approximately 45°, as the hardening coefficient decreases. Besides, in these cases, the yield zone size is very small compared with the width of the interface, so that these numerical examples belong to the small-scale yielding problem.

SMALL SCALE YIELDING PROBLEM

For small-scale yielding problem, it can be expected that the stress field out of the yield zone may be useful for strength evaluation. Fig. 9 shows the double logarithmic stress distribution out of the yield zone shown in Fig. 8 ($P = 30$ MPa) at the interface.

It can be found that the distributions are almost linear and parallel to each other, no matter what the hardening coefficient is. Therefore, the stress distribution outside the yield zone (i.e., in region III) can be written as:

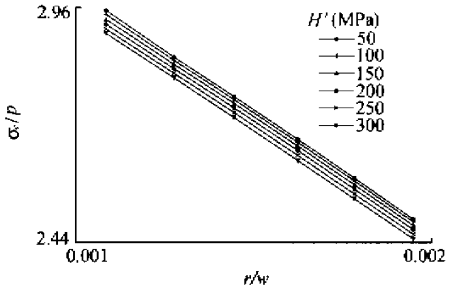

Fig. 9 Distributions of the effective stress on the interface outside the yield zone

$$\sigma_{ij} = \frac{Kf_{ij}(\theta)}{r^{1-\lambda}} \qquad r > r_s \tag{13}$$

where r_s is the radius of yield zone. The value of $1 - \lambda$ can be considered as not influenced by the hardening coefficient. Its numerical value can be obtained by the least square method. Table 3 shows the numerical results of λ. The singular order for the elastic interface edge (Bogy, 1971) is also shown in the table. It can be found that the value of λ is quite close to the elastic singular order no matter what value the hardening coefficient takes. This indicates that there is still an elastic singular stress field outside the yield zone near the interface edge, i.e., the elastic theory can be expected to be useful for the small-scale yielding problem. However, though the slope of the stress distribution for different hardening coefficients is the same, the value of the effective stress increases as the hardening coefficient decreases, as shown in Fig. 9. This fact means that the stress intensity is not the same for cases with different hardening coefficients (and so, is also different from that of the absolutely elastic case). The stress intensity factor K near the elastic interface edge for orthogonally bonded materials can be defined as (Xu and Jiang, 1998):

$$\sigma_\theta + i\tau_{r\theta} = \frac{K_1 + iK_2}{r^{1-\lambda}} \text{ at the interface} \tag{14}$$

Eq. (14) is also applicable for the elastic region (region III) in the small scale yielding case, by adding the condition of $r > r_s$. The stress inten-

sity factor then can be calculated by the extrapolation method based on Eq.(14). Table 3 shows the dimensionless numerical results of the stress intensity factor, in which the elastic solution is obtained by the absolutely elastic BEM analysis of the same model. It can be found that the stress intensity factor increases as the hardening coefficient decreases. Therefore, if the elastic solution of an interface edge is used to evaluate the strength of bonded dissimilar materials with small scale yielding region, some modification of the stress intensity factor is needed. However, it should be pointed out that this modification might depend not only on the hardening coefficient, but also the size of the yield zone (i.e., the loading).

Table 3 The slope of the stress distribution in region 3 and the dimensionless stress intensity factor under small scale yielding condition

H'(Mpa)	Elastic	1600	800	400	200	100	50
$1-\lambda$	0.2823	0.2823	0.2822	0.2823	0.2834	0.2848	0.2862
$K_1/(PW^{1-\lambda})$	0.5464	0.5528	0.5552	0.5575	0.5597	0.5617	0.5631

CONCLUSIONS

Through the theoretical analysis of the elastic-plastic singular stress field near the interface edge of bonded linear hardening materials, and elastic-plastic BEM analysis of the orthogonally bonded model, the following results were obtained:

1. The elastic-plastic singular stress field near an interface edge of bounded linear hardening material is substantially the same as that of elastic materials whose Young's modulus and Poisson ratio are substituted by equivalent values respectively.

2. The stress field near the interface edge of bonded linear hardening materials can be divided into three regions, i.e. the domain region of the elastic-plastic singular stress, the transitional region and the elastic region.

3. The domain region of the elastic-plastic singular field increases as the hardening coefficient increases. For materials whose $H'/E > 0.04$, the analogue analysis results based on the linearization of the strain-stress relation can be used. When $H'/E < 0.04$, the effective stress in most of the yield zone approximately equals to the yield stress.

4. The shape of the yield zone becomes thinner and longer, and the direction of the largest yield radius approaches to approximately 45°, as the hardening coefficient decreases.

5. For small-scale yield problem, the stress distribution outside the yield zone is almost the same as that of the elastic one, but the stress intensity factor increases as the hardening coefficient decreases.

References

Bogy, D.B., 1971. Two edge bonded elastic wedges of different materials and wedge angles under surface. *J. Appl. Mech.*, **38**: 377 – 389.

Brebbia, C.A., Telles, J.C.F., Wrobel, L.C., 1984. Boundary Element Techniques, In: Theory and Applications in Engineering, Springer-Verlag, London.

Champion, C.R., Atkinson, C., 1990. A mode III crack at the interface between two nonlinear materials. *Proc. R. Soc. Lond.*, **A 429**: 247 – 257.

Champion, C.R., Atkinson. C., 1991. A Crack at the Interface Between Two Power-Law Materials under Plane Strain Loading. *Proc. R. Soc. Lond.*, **A 432**: 547 – 553.

Gao, Y.L., Lou, Z.W., 1990. Mixed mode interface crack in a pure power-hardening bimaterial. *International Journal of Fracture*. **43**: 241 – 256.

Rudge, M.R.H., Tiernan, D.M., 1995. Interfacial stress singularities in a bimaterial wedge. *International Journal of Fracture*, **74**: 63 – 75.

Shih, C.F., Asaro, R.J., 1988. Elastic-plastic analysis of cracks on bimaterial interfaces: Part I-small-scale yielding. *J. Appl. Mech.*, **55**: 299

Shih, C.F., Asaro, R.J., 1989. Elastic-plastic analysis of cracks on bimaterial interfaces: Part II-structure of Small-scale Yielding Fields. *J. Appl. Mech.*, **56**: 763

Shih, C.F., Asaro, R.J., O'Dowd, N.P., 1991. elastic-plastic analysis of cracks on bimaterial interfaces: part III-large scale yielding. *J. Appl. Mech.*, **58**: 450

Xia, L., Wang, T.C., 1992. The interfacial crack between two dissimilar elastic-plastic materials. *Acta Mechanic Sinica*, **8**: 147 – 155

Xu, J.Q., Jiang, J.S., 1998. The Stress intensity factor for the crack near the interface Edge. *Shanghai Mechanics*, **19**(3): 221 – 228

Xu, J.Q., Muto, Y., 1999. Elasto-plastic stress singularity at interface edge with arbitrary boundary angles in dissimilar linear hardening materials. *Trans. of JSME* A65-**630**: 277 – 281.